RESIDUAL STRESSES IN OTSG TUBE EXPANSION TRANSITIONS

P.A. Sherburne, Framatome Technologies, Inc. D.J. Hornbach, Lambda Research
R.A. Ackerman, Toledo Edison Company A.R. McIlree, Electric Power Research Institute

ABSTRACT

A section of once through steam generator (OTSG) tubing, approximately 33 cm. long and encompassing the roll expansion region in the upper tubesheet (hot leg), was removed from the Davis Besse Nuclear Power Station in April 1996 for laboratory failure analysis. Rotating pancake coil (RPC) inspection of this region had determined that an axial defect was present in the expansion transition approximately 2.5 cm below the primary face of the hot leg tubesheet. Examination of the pulled tube section identified the defect as an ID-initiated primary water stress corrosion crack (PWSCC) approximately 78% throughwall and 2.3 mm long. Additional axial cracks with less throughwall extent were also observed within the roll transition.

During fabrication, OTSG's were subjected to a full-vessel stress relief at 593° - 621°C for ~12 to 15 hours. This practice was shown in early testing to reduce the residual stresses caused by roller expansion. Operating experience for OTSG tubing has demonstrated that it is more resistant to stress corrosion cracking than low temperature mill annealed Alloy 600 tubing used in early recirculating-type steam generators. Thus, the appearance of PWSCC in this tube was not expected.

A review of manufacturing records for the Davis Besse OTSG's revealed that this specific tube end had been repaired following stress relief and hydrotest operations. It was not clear from the records, however, if the tube had been rerolled as part of the repair procedure. Based on this uncertainty, a project was initiated to measure the residual stress distribution and cold work in the Davis Besse roll transition and in assorted rolled tube mockups, using X-ray diffraction techniques and finite element analysis. The objective was to determine if the Davis Besse tube had been rerolled following stress relief and thus more likely to experience PWSCC. Results confirm a definite effect of rerolling the tube following stress relief on both cold work and residual stresses. It was further concluded that the Davis-Besse tube data have a high degree of correlation with the reroll data.

Key words: Roller expansion, residual stress, stress corrosion cracking, Alloy 600

INTRODUCTION

Davis-Besse 1 is a 920 Mwe pressurized water reactor plant with two Model 177FA once through steam generators (OTSG's). Davis-Besse l began operating in 1977 and at Refueling Outage (RFO) 10 had accumulated 10.6 effective full power years (EFPY) of operation.

The Alloy 600 steam generator tubes are 0.625 inch (1.6 cm.) outside diameter with 0.034 inch (0.86 mm.) minimum wall thickness and are approximately 56 feet (~17 m) long. The tubes were installed during fabrication of the steam generators by inserting them through the tubesheet and tube support plate (TSP) holes, followed by rolling the tube ends into the upper and lower tubesheets to an engagement depth of 1 inch (2.54 cm). A full circumferential fillet weld was then added to the tubesheet joint to ensure a leak tight seal. After complete assembly, the entire generator was subjected to a furnace stress-relief heat treatment for the shell welds per ASME Code requirements. This heat treatment (593° - 621°C for ~12 to 15 hours) can also reduce the stresses in the expansion transition regions. Following stress relief, the vessels were hydrostatically tested. Any tube-to-tubesheet welds that leaked were repaired. This repair typically included a re-rolling step, which created a new non-stress-relieved transition deeper into the tubesheet (~2.3 inches (5.8 cm)).

During RFO 10, eddy current (EC) inspection was performed at the hot leg (upper) roll expansion transition for a group of eight steam generator tubes, which were reported as not having been stress-relieved. One of these eight tubes (tube 58/119) exhibited a single 0.2-inch (5 mm.) long axial indication at the roll expansion transition. However,

Eighth International Symposium on Environmental Degradation of Materials in Nuclear Power Systems – Water Reactors, Proceedings, August 10-14, 1997, Amelia Island, Florida, NACE, TMS

the roll transition was located approximately 1.3 inches (3.3 cm.) into the tubesheet. Since these data did not agree with the expected re-roll depth of ~2.3 inches (5.8 cm.), a review of the EC roll-depth data from the other seven tubes was performed, which revealed that all these tubes exhibited similar roll depths. A review of fabrication records indicated that the re-roll step was deleted from the repair procedure for the Davis-Besse OTSG's. Based on this information, it was assumed that roll expansion transitions in these eight tubes had been stress relieved, and therefore, were representative of the entire tube population. Additional EC inspections were then performed in the roll transition regions of 10% and 3.1% of the tubes in OTSG's "A" and "B," respectively. No additional indications were found.

Review of eddy current data for RFO 7 (1991 - 6.6 EFPY) and RFO 8 (1993 - 7.8 EFPY) for tube 58/119 showed an EC signature different from the signature of "typical" transitions; furthermore, the EC signature for tube 58/119 was essentially unchanged over this period of time. Remote dye-penetrant inspection detected a 0.03-inch (0.8 mm) long axial indication in the roll transition region. A 13-inch long section that included the roll expansion region in the upper tubesheet was subsequently removed from tube 58/119 for laboratory evaluation.

The laboratory examinations confirmed that the EC indication was caused by an ID-initiated stress corrosion crack within the roll expansion transition. The primary defect (Figure 1) was 2.3 mm long and ~78% throughwall and identified as primary water stress corrosion cracking (PWSCC). Additional degradation not detected during the field eddy current examination was also found within the roll expansion transition during the laboratory examination. This additional degradation included shallow intergranular attack and axial cracks with less throughwall extent than the primary defect.

It was subsequently postulated that tube 58/119 may have been rerolled to the original depth prior to repairing the weld. Based on this postulation, the next step in the overall investigation was to measure the residual stress distribution and cold work in tube 58/119. For comparison purposes, similar measurements were made in mockups that simulated both stress relieved and rerolled tube-to-tubesheet joints.

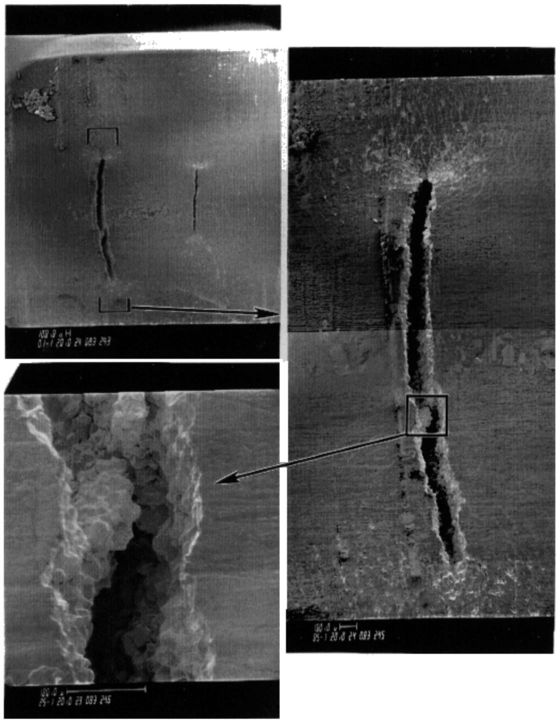

Fig. 1. – Primary defect (on left) in Davis-Besse Tube No. 58/119, after bending (10X)

EXPERIMENTAL PROCEDURES

Tube-to-Tubesheet Mockup Design

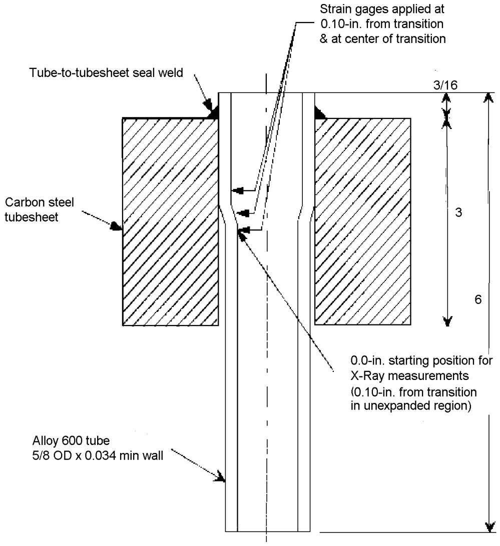

Fig. 2 – Mockup Specimen (typical)

EXPERIMENTAL AND ANALYTICAL PROCEDURES

Tube-to-Tubesheet Mockup Design

The typical mockup specimen consisted of a tubesheet block machined from carbon steel bar stock with one 0.625 inch (1.6 cm) OD x 0.034-inch (0.86 mm) minimum wall Alloy 600 tube rolled into it, to create the initial roll transition (Figure 2). The nominal dimensions of the tubesheet block were 1.5 inches (5.7 cm) OD by 3 inches (11.4 cm) long with a bore finish of 125 RMS or better. The mockup tubesheet block dimensions were selected to provide somewhat greater stiffness than the actual tubesheet to eliminate tubesheet distortion as a variable.

Composition and mechanical properties of the tubing material used for the mockup specimens were typical of commercial-grade Alloy 600. Yield strength of the mockup tubing was 54.7 ksi (377 MPa) as compared with 51.7 ksi (357 MPa) for the Davis-Besse tubing.

The tubes were rolled into the tubesheet using an Airetool #1219 three-roll expander tool with a fixed 0.1875-inch (4.8 mm) recessed thrust collar to assure that the tube protrudes 0.1875 inches from the face of the tubesheet. The rolls of this expander are 1.5 inches (3.81 cm) long with the last 0.25 inch (6.35 mm) of the roll rounded at a 1.0625 inch (2.7 cm) radius. The nose of the expander was set to a depth of 1.25 inches (3.18 cm) below the face of the tubesheet to assure a 1.0-inch (2.54 cm) effective roll. The expander was driven by an air motor set to shut off at a torque of 100 in-lbs. (1.15 kg-m). Lubricants were not used for the expansions.

Following roller expansion, the tube was manually welded to the tubesheet. The seal weld consisted of a 0.035-inch (8.9 mm) minimum throat fillet weld with the minimum length of both legs equal to 0.051 inches (1.3 mm).

Finally, the mockups were stress-relieved in a vacuum furnace to simulate the full vessel stress relief. Shop records indicate that the OTSG's were held at a stress relief temperature of 1100 (593 °C) to 1150 °F (621 °C) for 11 to 12 hours. Heatup and cool down rates were controlled to less than 20°F/hr (11.1°C/hr) due to control and OTSG structural limitations. For the mockups, heatup and cooldown rates were controlled to ≤20°F/hr (11.1°C/hr) above 600°F (316°C) only.

Four mockup specimens were fabricated to allow comparison of the range in possible residual stress levels with those of tube number 58-116:

Stress-relieved:	Two stress-relieved specimens, Cl and C2, represent nominal roll transitions in tubes that were subjected to full-vessel stress relief and placed in service without additional repairs performed.
Re-rolled:	Specimens Dl and D2 represent tubes that were rerolled following stress relief operations to the same depth as the original roll.

Strain Gaging and Sectioning

The mockup specimens were sectioned to provide access for the incident and diffracted x-ray beams. Before the specimens were sectioned, electrical resistance strain gage rosettes were applied on the inside diameter on both sides of the transition, and at the center of the transition region on each mockup, as shown in Figure 2. After the strain gages were attached, the tube was removed from the tubesheet by removing the seal weld (by milling) and sectioning the tubesheet away from the tube. The steel tubesheet block was slit axially using a narrow saw at 180° orientations, and the final web of material broken with wedges. The stress relaxation occurring on the OD surface of the tube resulting from tubesheet block removal was calculated using a finite element analysis (FEA) model and the stress relaxation data measured on the ID surface.

Following the OD residual stress measurements, the tubes were sectioned axially by electrical discharge machining (EDM). The strain relaxation due to sectioning was again recorded and used to correct the x-ray diffraction (XRD) residual stress measurements.

For the Davis-Besse tube segment, strain-gage rosettes were positioned on both the OD and ID as close as physically possible to the center of the roll transition zones. The gage rosettes on the tube OD and ID were measured to be 0.190 inch (4.8 mm) and 0.227 inch (5.8 mm), respectively, from the rolled end of the tube to the center of the gage. After the initial output voltages were recorded, the tube segment was sectioned along an axial plane ~45 degrees from the EC indication. Measured stress relaxations were less than ±5 ksi (34.5 MPa).

The total measured stress relaxations for the stress relieved specimens ranged from -2.5 ksi (-17.2 MPa) to +5.1 ksi (+35.2 MPa); whereas hoop stress relaxations on the order of +50 ksi (345 MPa) in the expanded region were measured for the rerolled specimens. The stress relaxation resulting from sectioning the tube to expose the inside diameter surface was relatively small compared to the stress relaxation from tubesheet removal for both specimens. The low stress relaxation for the stress relieved specimens is attributed to the effectiveness of the stress relief performed after initial roll expansion.

The small relaxation stresses measured for the stress relieved specimens and for the Davis-Besse tube segment were considered to be within the residual stress measurement accuracy and therefore not used to correct the measured residual stresses.

Profilometry

Prior to applying strain gages on the inside diameter of each tube, a silicon rubber casting compound was poured into the inside diameter of each of the mockup assemblies. The final mold was analyzed on an optical comparator at axial increments of 0.040 inch (1 mm). After the tubesheet blocks were removed, the radial profiles were measured as a function of axial displacement on the outside diameter of each of the four specimens. The displacements were measured with an indicator resolution of 1×10^{-4} inch (2.5 μm).

X-Ray Diffraction Residual Stress Measurements

X-ray diffraction provides a tool for determining both the macroscopic residual stress field and estimated degree of cold work through the transition region of tube to tubesheet expansion transitions. Measurements were performed using a two-angle sine-squared-psi technique, employing the diffraction of manganese K-alpha radiation from the (311) planes of the FCC structure of Alloy 600. Details of the measurement technique and equipment used are discussed in Reference 1.

Residual stress measurements were taken on the outside and inside diameters of all five specimens as a function of distance from the transition region and depth into the wall. Measurements were made in the hoop and axial directions at 0.050-inch (1.3-mm) increments over a 0.45-inch (11.4-mm) range centered on the transition zone. The measurements were made at the surface and at depths of 1 and 3×10^{-3} inch on both the outside and inside diameters. A l x 2-3 mm rectangular irradiated area was used to include a statistically significant number of grains for meaningful measurement of the residual macrostresses while providing the necessary spatial resolution to profile the axial stress distribution.

Material was removed electrolytically for subsurface measurement, minimizing possible alterations of the subsurface residual stress distribution. All data obtained as a function of depth were corrected for the effects of the penetration of the radiation employed for residual stress measurement into the subsurface stress gradients and for relaxation caused by both sectioning and metal removals.

The percent cold work was determined from the half width (B1/2) of the (311) diffraction peak from the data obtained in the psi=0 orientation for residual stress measurement. The K-alpha l diffraction peak width was separated from the superimposed K-alpha doublet, assuming a Pearson VII function diffraction peak profile. The percent cold work was calculated from the diffraction peak half width based upon an empirical relationship established using specimens deformed to known levels of true plastic strain. The percent cold work is reported as a scalar quantity, and represents the true plastic strain required to produce the diffraction peak width measured, based upon the empirical relationship.

Finite Element Analysis (FEA)

A non-linear finite element model of the Alloy 600 tube was made in order to study the effect of yield strength gradients caused by cold working of the outer diameter skin during grinding. The primary purpose of the nonlinear FEA tube model was to demonstrate the influence of a shallow layer of cold worked outside diameter material on the final residual stress field following roller expansion. The conversion of the (311) peak width data to the equivalent cold work in the first 0.001 inch (35.4 μm) of material on the outside surface indicated the surface was cold worked as much as 50 percent, during the fabrication process. The yield strength of the material will subsequently rise as a result of the cold working, and was estimated from the percent cold work results and available true stress-strain curves for Alloy 600. The yield strength gradients were built into the FEA model to account for variations in material properties caused by prior cold working. The tube FEA model was plastically deformed radially to imitate the primary deformation occurring during the rolling operation.

RESULTS

OD surface residual stress measurements were taken on stress-relieved specimen C1 at orientations of 0, 90, 180, and 270° to determine rotational symmetry of the stress distribution. Results, plotted in Figure 3, show little variation in either axial or hoop stress as a function of angular position. This rotational symmetry was assumed to apply to the remainder of the specimens, and all further residual stress measurements were made in one plane only.

Residual stress data and cold work for stress-relieved specimen Cl are shown in Figures 4 and 5. For this specimen, the residual stresses on the OD of the tube are, in general, compressive in the unexpanded region in both the hoop and axial directions, becoming less compressive through the expansion transition. ID residual stresses tend to mirror the OD residual stresses, decreasing through the expansion transition from around 25 ksi (172 MPa) tension in the unexpanded region to ~25 ksi (~172 MPa) axial compression and nearly 0 to slight tension in the hoop direction in the fully expanded region. These stresses are significantly less than yield strength (~55 ksi). Based on only these stresses, SCC in the primary water environment would not be expected. It must be noted, however, that operating stresses must be added to the residual stresses to obtain the true stress distribution through the transition.

The results indicate cold working induced by the roller expansion process on both the OD and ID surfaces. Percent cold work on the ID varies from ~20 percent at the surface in the fully expanded region to between 5 and 10 percent below the surface. The percent cold work varies between 20-30 percent at the OD surface, decreasing to <5 percent at a depth of 0.001 inch (25.4 μm). This compares to ~50 percent surface cold work for the as-received Alloy 600 tube used in fabricating the mockups (Figure 6). This thin cold-worked layer is presumably the result of centerless grinding and/or rotary straightening operations performed in the tube mill. The as-received tubing also demonstrated surface tension, in the hoop direction, of ~20 ksi (140 MPa), and axial compression to a depth of ~0.003 inches (76.2 MPa). This indicates that both the residual stresses and the surface cold work has been significantly decreased as a result of the furnace stress relief.

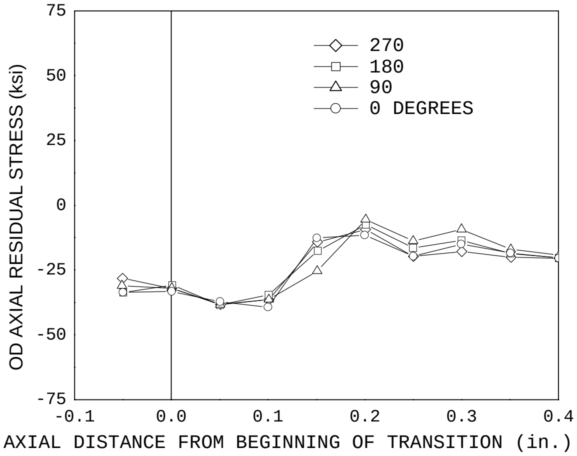

(a) axial residual stress distribution

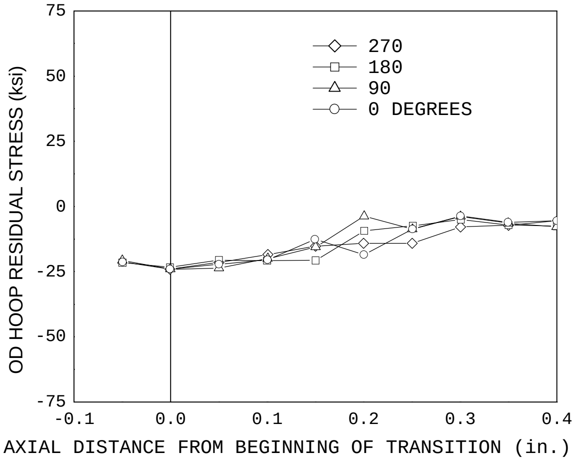

(b) hoop residual stress distribution

Fig. 3 – Circumferential variation of OD residual stresses for a stress-relieved mockup

As might be expected, the specimens rerolled after stress relief exhibit much higher residual stresses and percent cold work (Figures 7 and 8). The OD axial stresses vary from 50 ksi (345 MPa) tension at a depth of 0.003 inch (76.2 μm) in the fully expanded region, to ~65 ksi (448 MPa) compression at the tail of the expansion. Hoop stresses remained compressive through the length of the specimen. For the rerolled specimens, OD circumferential cracking might be expected at the end of the expansion and beginning of the transition. This is, in fact, where circumferential ODSCC has occurred in recirculating steam generators[4] and in tubing installed in a model boiler without stress relief.[5]

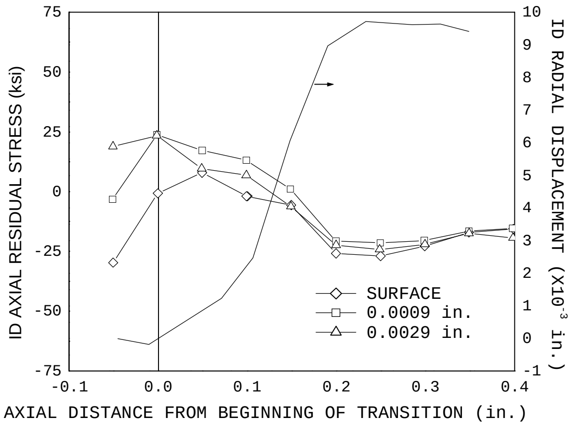

(a) axial residual stress distribution

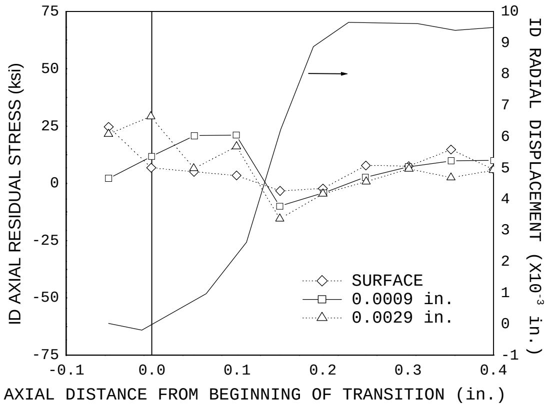

(b) hoop residual stress distribution

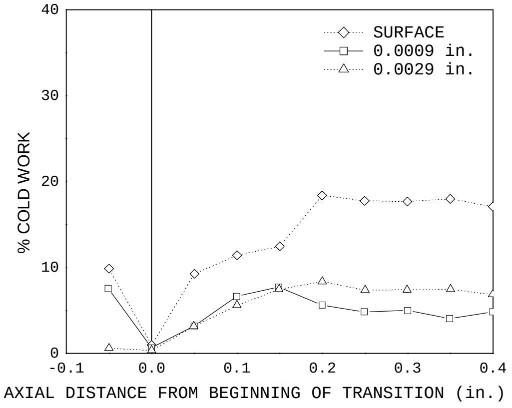

(c) cold work distribution

Fig. 4 – ID residual stresses and cold work for a stress-relieved mockup.

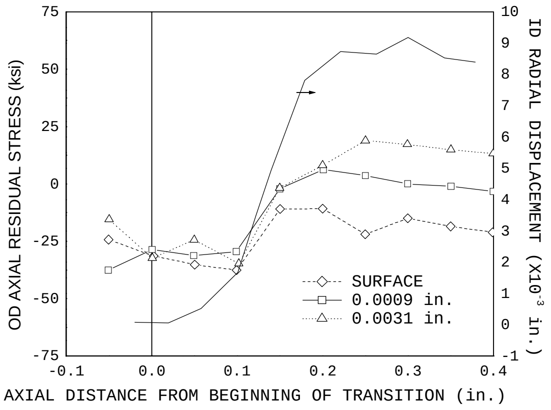

(a) axial residual stress distribution

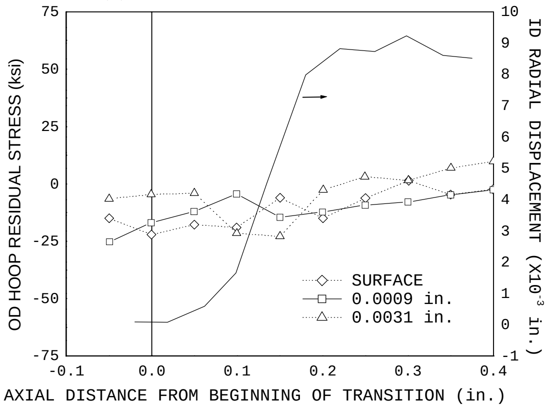

(b) hoop residual stress distribution

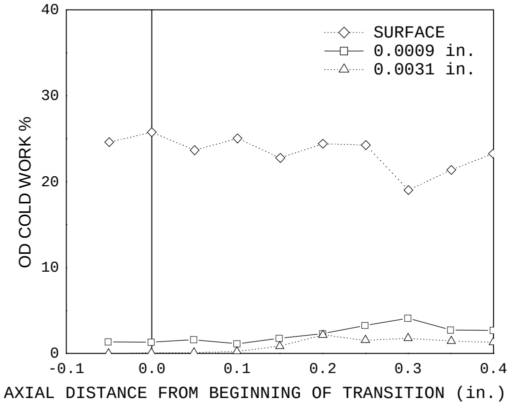

(c) cold work distribution

Fig. 5 - -OD residual stresses and cold work for a stress-relieved mockup

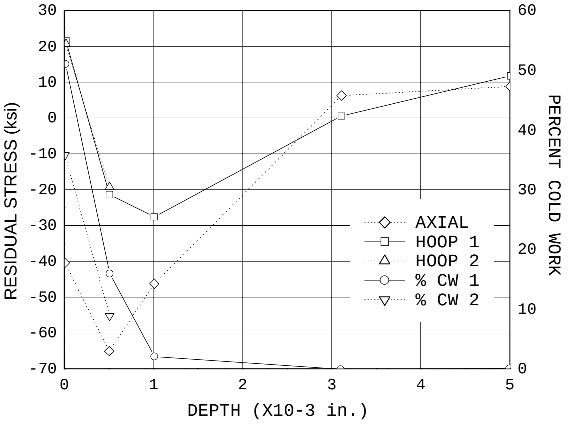

Fig. 6 – OD residual stress and cold work distribution for as-received Alloy 600 tube

ID residual stresses in the rerolled specimens are as high as the tube yield strength (50 - 60 ksi (345 MPa - 414 MPa) tension) at the end of the expansion transition (near the unexpanded end) in both the axial and hoop directions. Percent cold work is as high as 50 - 70 percent over much of the expansion transition and remains at 30 percent at a depth of 0.003 inch (76.2 µm). For these specimens, both axial and circumferential SCC would be expected at the end of the transition.

The residual stress measurements for the Davis-Besse tube segment (Figure 6) exhibit more data scatter than do the mockup specimens, presumably due to both tube removal trauma and ID corrosion. The OD axial and hoop stresses, all compressive, are similar in magnitude to the rerolled specimens, although the OD percent cold work is smaller (15 - 25 percent vs 25 - 30 percent). The ID exhibits significant tensile stresses in the axial direction nearer the unexpanded end of the expansion transition, while the ID hoop stresses vary from -25 ksi to +40 ksi (-172 MPa to +276 MPa) in the expansion transition. The Davis-Besse residual stress measurements, however, were not corrected for the relaxation stresses that might have occurred as a result of removal from the tubesheet, since these values are unknown. If the correction made for the rerolled specimens were to be applied to the Davis-Besse tube section, then the ID hoop stresses could be compressive through the expansion transition. On the basis of residual stress alone, IGSCC would not be expected in the region in which it occurred.

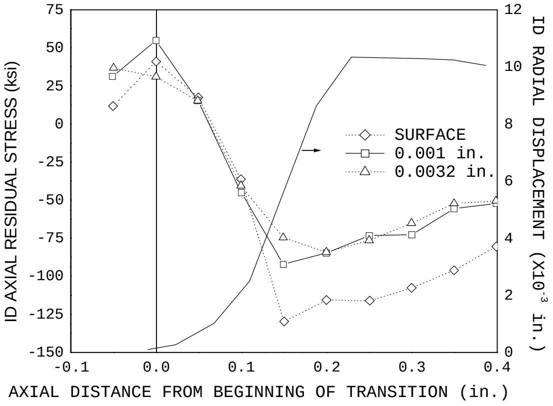

(a) axial residual stress distribution

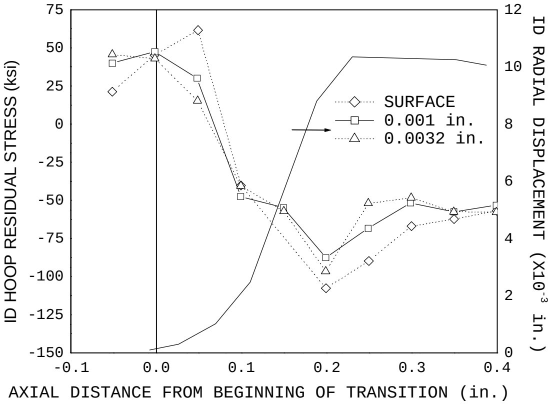

(b) hoop residual stress distribution

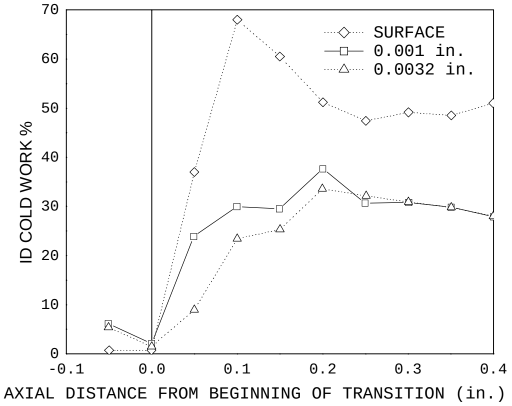

(c) cold work distribution

Fig. 7 – ID residual stresses and cold work for a rerolled mockup

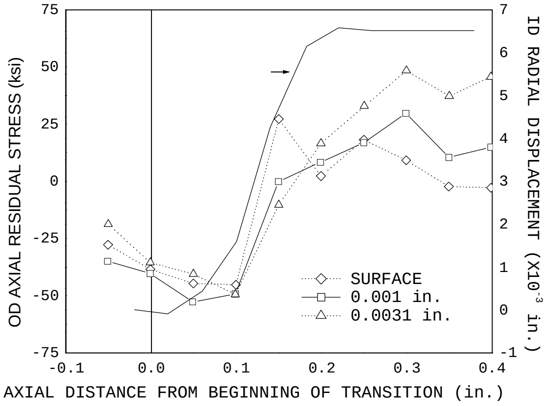

(a) axial residual stress distribution

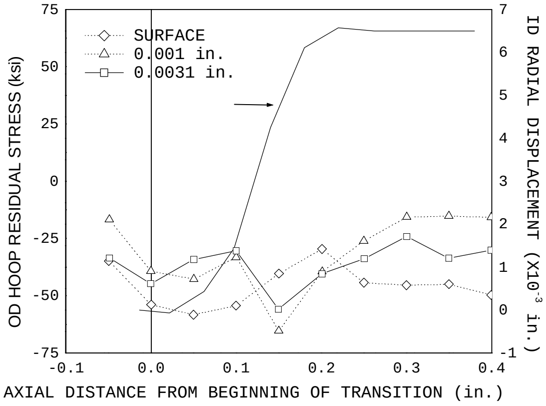

(b) hoop residual stress distribution

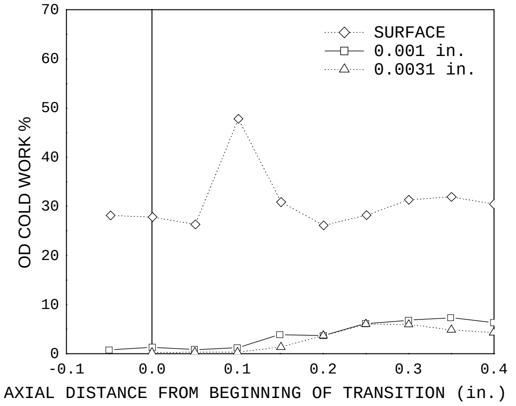

(c) cold work distribution

Fig. 8 – OD residual stresses and cold work for a rerolled mockup.

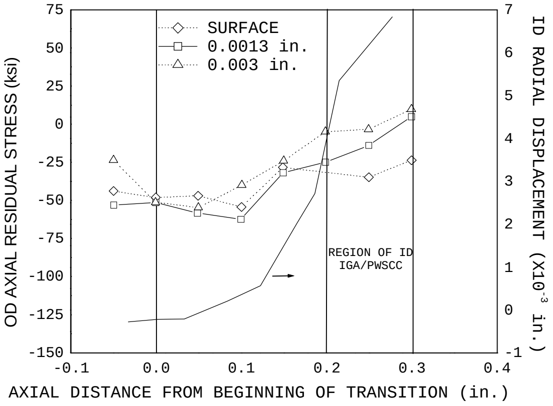

(a) axial residual stress distribution

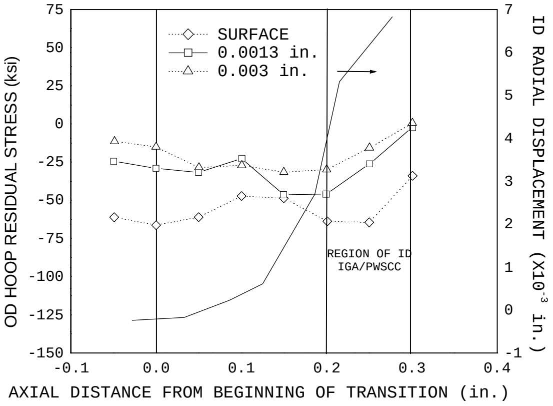

(b) hoop residual stress distribution

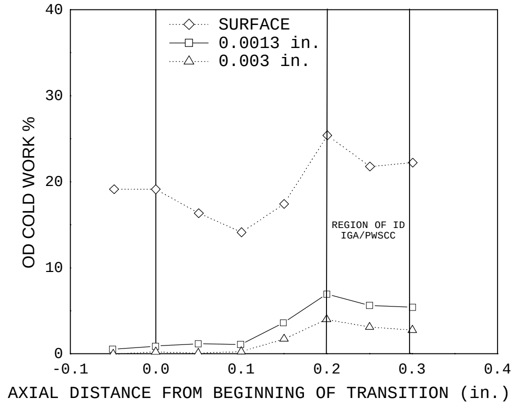

(c) cold work distribution

Fig. 9 – OD residual stresses and cold work in the expansion transition of the Davis-Besse pulled tube segment.

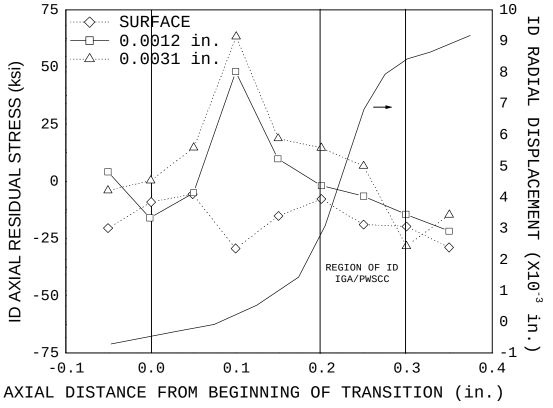

(a) axial residual stress distribution

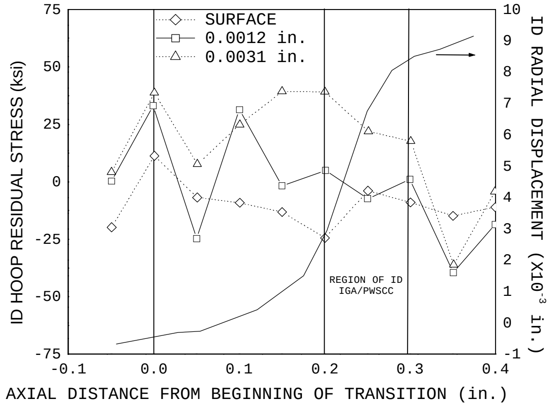

(b) hoop residual stress distribution

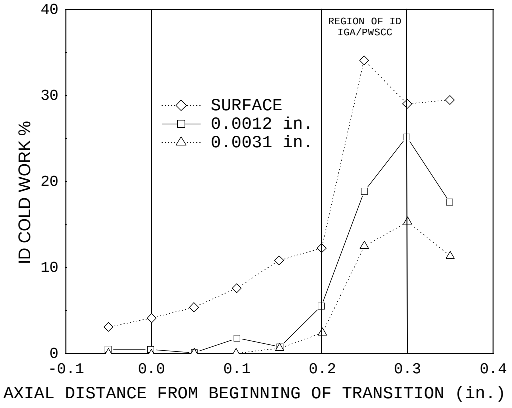

(c) cold work distribution

Fig. 10 – ID residual stresses and cold work in the expansion transition of the Davis Besse pulled tube segment.

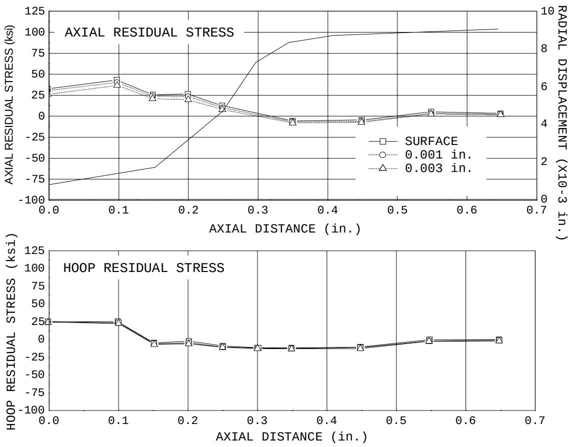

Fig. 11 – Inside diameter FEA residual stress distribution. Alloy 600 OTSG tube finite element model, ID location.

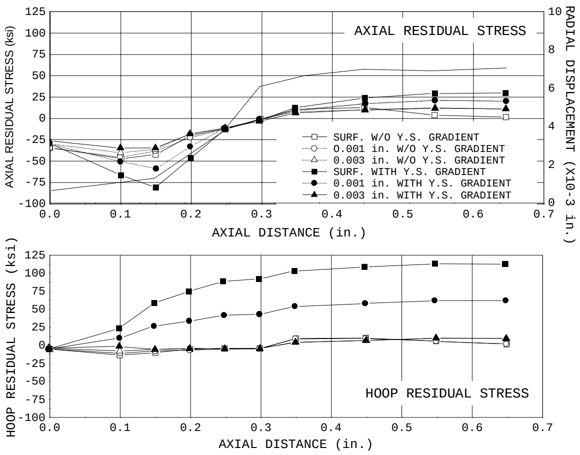

Fig. 12 – Outside diameter FEA residual stress distribution. Alloy 600 OTSG tube finite element model, OD locations.

The percent cold work on the ID of the Davis-Besse tube in the region in which IGA/IGSCC occurred (30 - 34 percent) is between the peak values for the stress-relieved specimens (18 - 22 percent) and the rerolled specimens (50 - 70 percent).

Microhardness measurements made on longitudinal cross sections indicate an increase in hardness in the transition and fully-expanded zones of both the stress-relieved and rerolled specimens, which is attributed to cold working of the tubing during roll expansion. Both specimens show maximum hardness near the inside surface, the point of contact with the rollers. The axial location for, and maximum values of, microhardness are given in Table I. For all three specimens, the position of peak microhardness values is near the center of the expansion transition. As may be seen in Table I, microhardness decreases from the ID, where the rollers contact the tubing, to the OD for both the rerolled specimen and the Davis-Besse tube segment. The microhardness changes very little from the ID to the OD for the stress relieved specimen. This data tends to support the premise of reroll for the Davis-Besse tube.

TABLE I – Microhardness Measurements

Specimen	Position from Start of Transition* (inches)	Knoop Microhardness (HKN)		
		OD	Mid-wall	ID
C1 (stress-relieved)	0.14	253	259	256
D1 (rerolled)	0.14	253	265	310
Davis-Besse	0.13	244	247	280

* as measured from unexpanded end

As noted earlier, relaxation stress corrections due to removal of the tubesheet blocks were significant (on the order of +50 ksi hoop stress) for the rerolled mockups and negligible (<5 ksi hoop stress) for the stress-relieved mockups. This implies that the furnace stress relief apparently relieved a significant amount of the contact pressure between the tube and tubesheet. The analysis indicated that the contact pressure for the rerolled mockups was ~5300 psi, whereas, for the stress-relieved mockups, the contact pressure was only 500 psi.

Finite Element Analysis

The finite element calculated OD residual stress results for the tube model without the yield strength gradient, shown in Figure 11, indicate similar trends and magnitude of the calculated residual stresses to those measured for the stress relieved mockups. The model which includes the outer surface yield strength gradient caused by machining operations seems to show better agreement in axial residual stress distribution in the fully expanded zone than the model without the gradient. The OD hoop residual stress results indicate a marked difference in residual stresses between the models with and without the yield strength gradient. The surface tensile stresses are an order of magnitude higher in the expanded region when the yield strength gradient is included.

The ID surface FEA residual stress results for the tube model are shown in Figure 12. The results show good agreement with the x-ray diffraction results obtained on the ID of the stress relieved mockups.

CONCLUSIONS

Results of this project confirm a definite effect of rerolling the tube following stress relief on both cold work and residual stresses. The ID surface cold work and microhardness values for the Davis-Besse tube section lie between the stress relieved and the rerolled specimens, which would be in the direction of supporting the reroll. If, however, the measured stresses were corrected for the presumed insitu contact pressure using the same relaxation correction applied to the rerolled specimen, the ID residual stresses would be compressive through the roll transition. The effect of the IGA/IGSCC and tube removal operations on the measured residual stresses for the Davis-Besse tube segment is unknown, however.

Based on the above discussion of results, it is concluded that the Davis-Besse tube data has a high correlation with reroll data. This high correlation is a sufficient demonstration that the Davis-Besse tube was rerolled to the same depth following stress relief.

ACKNOWLEDGMENTS

This research was sponsored by the B&W Owners Group.

REFERENCES

1. P. Prevéy, "X-Ray Diffraction Residual Stress Techniques," Metals Handbook, 10, Metals Park: ASM, 1986, pp. 380-392.
2. D. P. Koistinen and R. E. Marburger, *Trans. ASM*, Vol. 51, 1959, pp. 537-550.
3. M.G. Moore and W.P. Evans, Trans. ASM, Vol. 66, 1958, pp.340-345.
4. Steam Generator Reference Book, EPRI TR-103824, Revision I, December 1994, pp.12-52.
5. J.L. Barna and L.W. Sarver, Intergranular Attack or Corrosion in a Once-Through Model Steam Generator, EPRINP-5120, July 1987.